JOURNAL OF NANO- AND ELECTRONIC PHYSICS
Vol. **5** No 2, 02030(5pp) (2013)

ЖУРНАЛ НАНО- ТА ЕЛЕКТРОННОЇ ФІЗИКИ
Том **5** № 2, 02030(5cc) (2013)

Evidence of Itinerant Ferromagnetism in Transition Metal Doped ZnO Nanostructures

V. Bandyopadhyay, K. Bhushan, S. Mukherjee*

Department of Applied Physics, Birla Institute of Technology, Mesra, Ranchi – 835215 Jharkhand, India

(Received 15 February 2013; published online 04 May 2013)

This work is aimed at synthesizing and characterizing transition metals (Mn, Fe and Ni) doped ZnO nanostructures. The samples have been prepared by chemical co-precipitation method. The samples have been divided and one half has been coated SiO_2. X-Ray diffraction indicated the formation of single phase ZnO. Optical and photoluminescence studies have been carried out using UV-Vis spectroscopy and Photoluminescence spectroscopy respectively. Magnetic responses of the samples have been studied using SQUID. The structural studies revealed that sample is having wurzite structure at room temperature. Magnetization results shows the ferromagnetism in 2 % Fe doped, 5 % Ni doped and 2 % Mn doped ZnO.

Keywords: ZnO, Dilute magnetic semiconductors, Co-precipitation, Ferromagnetism, Superconductivity.

PACS number: 75.50.Pp

1. INTRODUCTION

Diluted magnetic semiconductors (DMS) have recently attracted huge research attention because of their potential application for spintronics devices. In DMS materials, transition or rare earth metal ions are substituted onto cation sites and are coupled with free carriers to yield ferromagnetism via indirect interactions. ZnO based DMS is particularly interesting since it shows interesting spintronics property at room temperatures. There has been a lot of interest in doping ZnO with 3d transition metal ions, since the prediction made by Dietl et al. [1] that Mn-doped ZnO would be ferromagnetic at room temperature. Magnetic impurities, like transition metals, can make the semiconductor half-metallic: the majority spin bands are metallic and the minority spin bands are semiconducting; as a result, the compound presents a fully (100 %) spin polarized density of states (DOS) at the Fermi energy, and this property is used in electronic industries to build spintronics devices [2].

ZnO is a of II-VI compound semiconductor of the periodic table whose ionicity resides at borderline between covalent and ionic semiconductor [3]. The electronegative difference between zinc and oxygen produce a high degree of ionicity in its bond. Considering that the n-type ZnO is easily available and the intrinsic defects such as the O-vacancies and Zn- interstitial work as donor it can be concluded that the (Zn, Fe)O, (Zn, Co)O and (Zn, Ni)O are promising candidates for achieving high-T_C ferromagnetism.

2. EXPERIMENTAL

Transition metal doped ZnO nanostructures were synthesized by chemical co-precipitation method [4-7]. We have prepared three series of samples of generic formula $Fe_xZn_{(1-x)}O$, $Ni_xZn_{(1-x)}O$ and last one of $Mn_xZn_{(1-x)}O$ where x is 0.02 and 0.05. In each case, one sample is coated with SiO_2 and another is left uncoated. For the synthesis of all the samples, Zinc nitrate hexahydrate ($N_2O_6Zn.6H_2O$), Iron(III)nitrate nonahydrate($FeN_3O_9.9H_2O$), Nickel(II)nitrate hexahydrate($N_2NiO_6.6H_2O$), Manganese(II)Chloride ($MnCl_2$) and sodium Hydroxide (NaOH) were used which are procured from Sigma Aldrich. Tetra ethyl orthosilicate (TEOS) was used for coating the nanocrystals formed by solution method. For synthesis of the first series of generic formula $Fe_xZn_{(1-x)}O$, calculated weights of salts of Zn for forming ZnO host and as well as Fe as dopants were dissolved in methanol at room temperature to produce a solution with a total concentration of metal ions of 0.1 M. A solution of NaOH in methanol was used as the precipitating agent and was added dropwise to the solution in a temperature of 80 °C. This thermal condition also favors the reduction of the metal ions to metal clusters, leading to a composite material formed mainly by doped zinc oxide decorated with metal clusters. These clusters appear to be the main species responsible for the ferromagnetism of the Fe doped zinc oxide. Thus, by this process, the ferromagnetism is a result of extrinsic character rather than an intrinsic one [8]. To achieve adequate precipitation, the alkali solution was added until the pH of the solution with metal ions reach 10.

When reaction was completed, the precipitate was separated from the supernatant by centrifuge machine operating at a speed of 1500 rpm, and washed several times with ethanol and then dried at room temperature. The precipitated part is then divided into two parts; one part is coated using TEOS (tetra ethyl orthosilicate) and dried at the room temperature. For the second series of generic formula $Ni_xZn_{(1-x)}O$, salts of Zn and Ni were used and similarly for the third one of $Mn_xZn_{(1-x)}O$ with Zn and Mn. The remaining steps were same as that of the first series of samples.

3. RESULTS AND DISCUSSION

3.1 X-Ray Diffraction

Structural analysis of transition metal doped ZnO nanoparticles was performed in an X ray diffractometer (XRD) using CoK_α ($\lambda = 1.788$ nm). XRD patterns of all the samples of the series of doped ZnO nanocrystals were shown in Fig. 1a, b and c. The sharp intense peaks originated from (100), (002), (101), (102), (110), (103), (200) in all the samples confirms the good crys-

* samrat.udc@gmail.com

talline nature of würtzite-type ZnO [9]. The average crystallite sizes (D_{av}) were estimated by using the Debye-Scherrer equation [10] in our experiment.

$$D_{av} = \frac{0.9\lambda}{\beta_{1/2}\cos\theta}$$

In the above equation, λ represents the wavelength of the X-ray radiation, $\beta_{1/2}$ the full width at half maximum of the diffraction peak (in radians) and θ the maximum scatter angle.

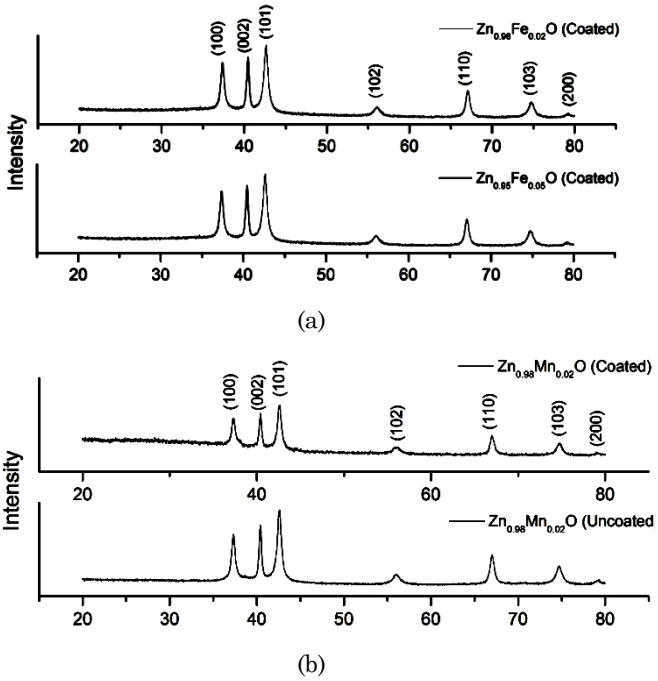

Fig. 1 – XRD Representative patterns of transition metal doped ZnO Nanostructures: Series of generic formula $Fe_xZn_{(1-x)}O$ (a), Series of generic formula $Mn_xZn_{(1-x)}O$ (b).

Table 1 – Average particle size estimated from the diffraction spectrum in Fig. 1 by using FWHM

Sample Name	Type of Particle	2θ	FWHM (β) in radians	Average size of the particle (nm approx)
$Fe_{0.02}Zn_{0.98}O$	Coated	38.25	0.021	24
	Uncoated	38.46	0.025	21
$Fe_{0.05}Zn_{0.95}O$	Coated	40.00	0.022	24
	Uncoated	38.46	0.021	25
$Ni_{0.02}Zn_{0.98}O$	Coated	37.36	0.013	36
	Uncoated	38.64	0.021	25
$Ni_{0.05}Zn_{0.95}O$	Coated	37.33	0.005	97
	Uncoated	38.89	0.019	28
$Mn_{0.02}Zn_{0.98}O$	Coated	37.39	0.019	27
	Uncoated	37.36	0.009	51
$Mn_{0.05}Zn_{0.95}O$	Coated	37.36	0.011	65
	Uncoated	37.36	0.016	46

We use the (101) peak in the XRD patterns to calculate the average crystallite size. From Table 1 we can clearly observe that the particle size of the coated sample is larger as compared to the uncoated samples, this is due to the coating of amorphous silicon dioxide around the particles resulting in increased size. The absence of any extra peak in the XRD of Mn and Ni doped ZnO suggests that the actual incorporation of dopant species into the ZnO structure. A higher baseline is observed in case of all coated samples, this can be explained as the formation of amorphous silicon dioxide due to coating.

3.2 UV-Visible Spectroscopy

Optical analysis of the doped ZnO nanoparticles was performed by an Ultraviolet-visible spectroscopy in the region from 200 nm to 800 nm at room temperature. Fig. 2a, b and c shows spectrum of absorption versus photon energy of the samples.

The estimated band gap value of ZnO is approximately 3.3 eV for the nanoparticle [11], and one can observe that the band gap changes due to doping the transition metal in ZnO. The systematic shifts with doping levels suggest that it is due to the introduction of dopant ions, rather than size effects which brings these changes. This is further corroborated due to the fact that the sizes of the nanoparticles are well above the confinement region. A number of previous experimental and theoretical investigations have suggested that size effects have little or no influence on the band structure of ZnO nanocrystals with diameters greater than 7.0 nm [12]. In our experiment here the XRD results is showing the size greater than 7.0 nm therefore we have to drop that reason of size for the increment of the band gap rather is due to the doping of transition metal.

The bandgap was calculated by differentiating the as obtained graphs and the higher wavelength side was considered. The was done because the first change in slope indicates the onset of the valence to conduction band edge transition.

Table 2 enlists the bandgap of all the samples of transition metal doped ZnO nanostructures.

Table 2 – Estimated band gaps of the samples

Sample Name	Type of Particle	Peak at Wavelength (nm)	Bandgap (eV)
$Fe_{0.02}Zn_{0.98}O$	Coated	372	3.33
	Uncoated	373	3.32
$Fe_{0.05}Zn_{0.95}O$	Coated	369	3.36
	Uncoated	373	3.32
$Ni_{0.02}Zn_{0.98}O$	Coated	376	3.30
	Uncoated	379	3.27
$Ni_{0.05}Zn_{0.95}O$	Coated	351	3.53
	Uncoated	376	3.29
$Mn_{0.02}Zn_{0.98}O$	Coated	369	3.36
	Uncoated	371	3.34
$Mn_{0.05}Zn_{0.95}O$	Coated	342	3.63
	Uncoated	364	3.41

3.3 PL Spectroscopy

Photoluminescence analysis of the doped ZnO nanostructures were performed at room temperature from the dispersed particles in methanol. Xenon lamp source at an excitation wavelength of 280 nm is used for the analysis. Photoluminescence and absorption in semiconductors

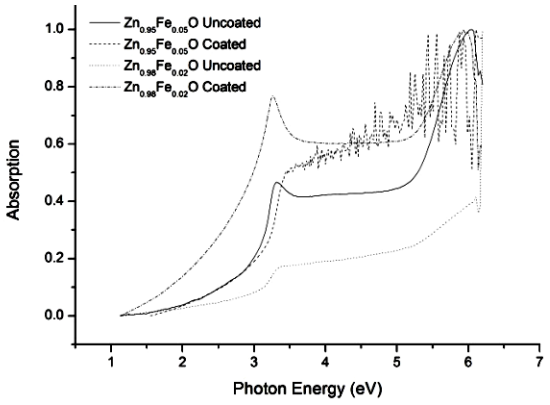

(a)

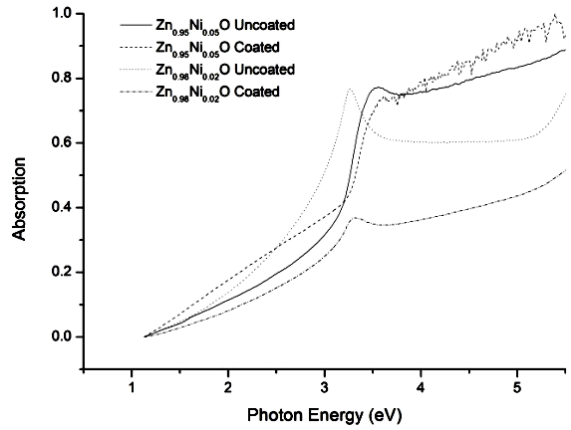

(b)

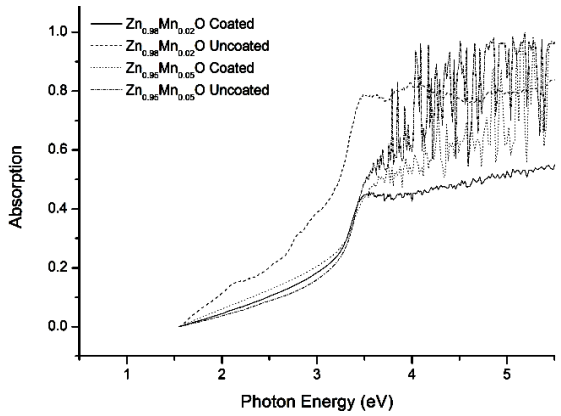

(c)

Fig. 2 – UV-Vis patterns of transition metal doped ZnO Nanostructures: Series of generic formula $Fe_xZn_{(1-x)}O$ (a), Series of generic formula $Ni_xZn_{(1-x)}O$ (b), Series of generic formula $Mn_xZn_{(1-x)}O$ (c)

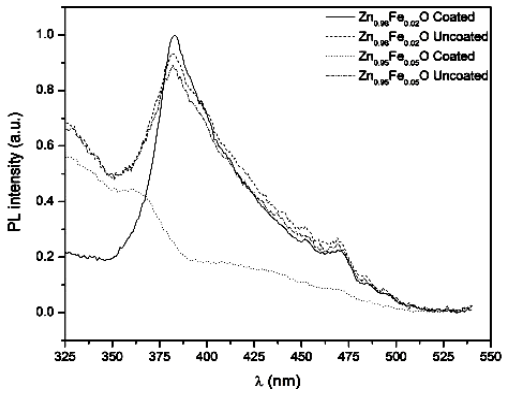

(a)

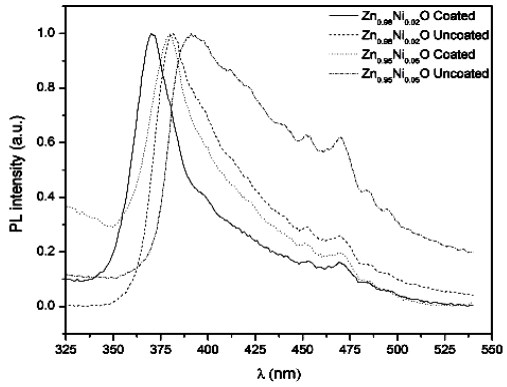

(b)

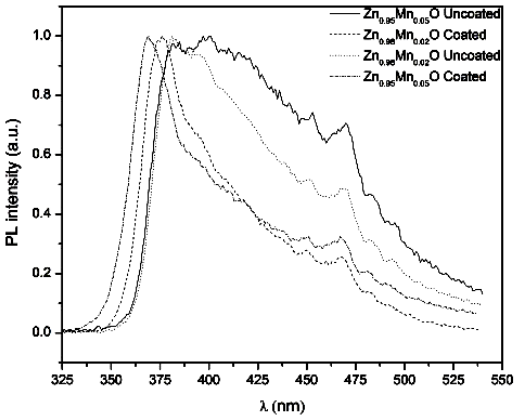

(c)

Fig. 3 – PL Spectra of transition metal doped ZnO Nanostructures: Series of generic formula $Fe_xZn_{(1-x)}O$ (a), Series of generic formula $Ni_xZn_{(1-x)}O$ (b), Series of generic formula $Mn_xZn_{(1-x)}O$ (c)

strongly relies on the assumption that the recombination times are much larger than the intraband relaxation times.

The energy of a donor-acceptor pair in bulk ZnO can be calculated as:

$$E_{DAP} = E_g - E_D^{\text{Bind}} E_A^{\text{Bind}} + e^2 / 4\pi\varepsilon\varepsilon_0 R_{DA} \qquad (13)$$

where Eg is the band gap (distance between conduction and valence bands), which is 3.437 eV at 2 K, E_D^{Bind} is the binding energy of donor (energy below the bottom of conduction band), E_A^{Bind} is the binding energy of an acceptor (energy above the top of valence band), ε_0 is the permittivity of free space, e is the electron charge, ε is the dielectric constant and R_{DA} is the donor-acceptor pair separation. The photoluminescence spectra of the three sets of samples are shown in Fig. 3a, b and c.

Considering the spectral information of all the samples, strong peaks ranging from 370 nm to 391 nm were observed. A typical ZnO UV-exitonic emission band around 380 nm is observed, which is the characteristics of band edge emission. On being exposed to 280 nm radiation the prepared samples emits visible blue line. This visible emission is also evident from the photoluminescence graph as shown in Fig. 3.

Table 3 – Emission Wavelength by PL Emission Spectra

Sample Name	Type of Particle	Peak at Wavelength (nm)
$Fe_{0.02}Zn_{0.98}O$	Coated	383
	Uncoated	382
$Fe_{0.05}Zn_{0.95}O$	Coated	360
	Uncoated	382
$Ni_{0.02}Zn_{0.98}O$	Coated	370
	Uncoated	381
$Ni_{0.05}Zn_{0.95}O$	Coated	380
	Uncoated	391
$Mn_{0.02}Zn_{0.98}O$	Coated	385
	Uncoated	382
$Mn_{0.05}Zn_{0.95}O$	Coated	378
	Uncoated	372

3.4 Magnetization Measurements

The magnetization responses of all the uncoated samples were studied in a SQUID (Quantum Design). The M-H responses of the samples are shown in Fig. 4a, b and c.

The sample doped with Mn shows the highest magnetic response whereas for Fe and Ni the response is extremely weak. The coercivity obtained for the samples and varies from 114 Oe to 189 Oe which is definitely more than other reports [15]. The ferromagnetic nature cannot be a consequence of metal-metal interaction because the medium in which the samples have been prepared do not have any reducing properties. The ferromagnetic behaviour observed in the samples is probably due to competition between the double-exchange interaction and the antiferromagnetic

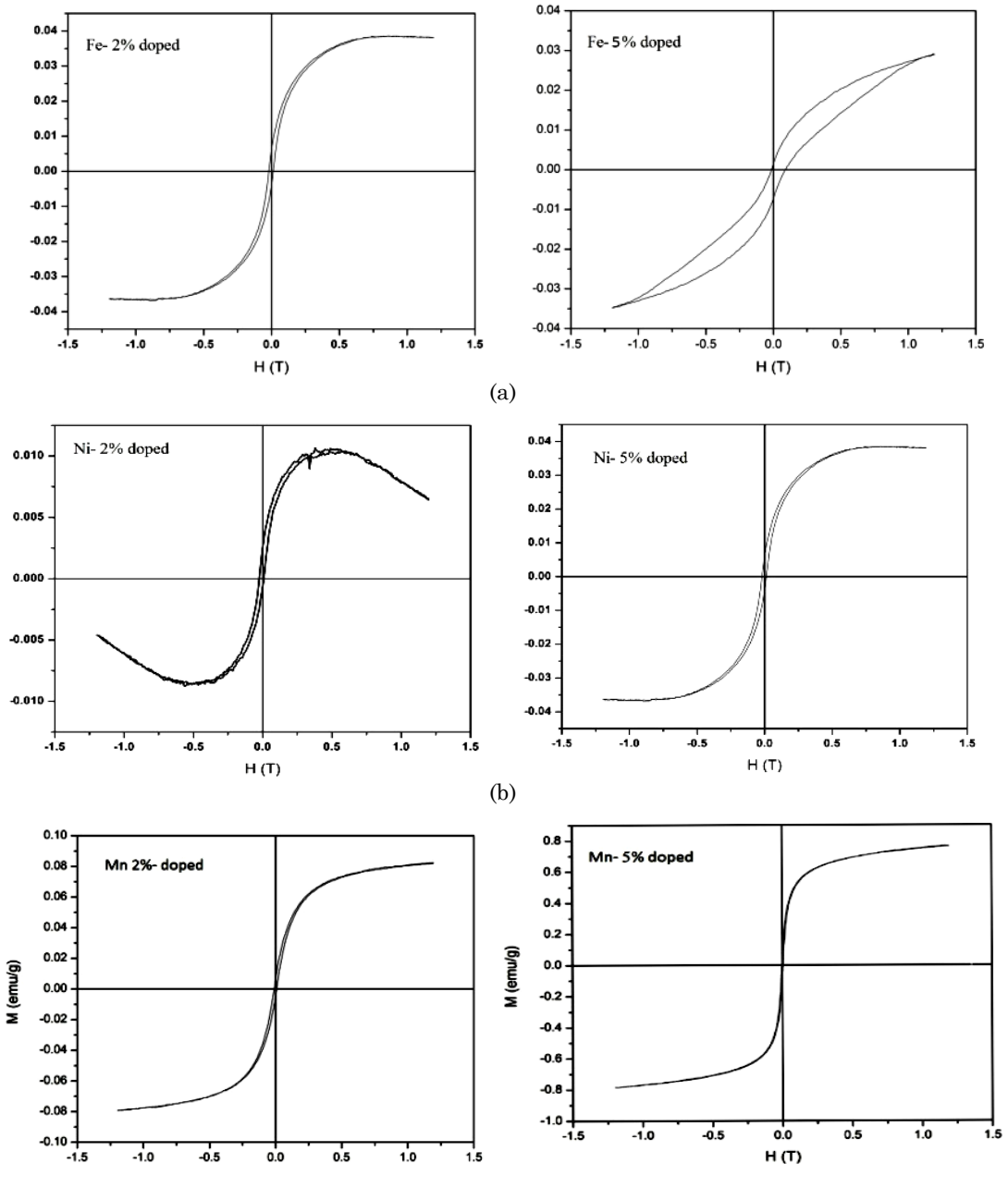

Fig. 4 – M-H curve at room temperature of Fe doped ZnO nanostructures (a), Ni doped ZnO nanostructures (b), Mn doped ZnO nanostructures

superexchange interaction in the material. The low magnetization and coercivity values measured for our samples are standard properties of nanocrystalline dilute magnetic semiconductors. Radovanovic [16] suggested the formation of dense aggregates of Ni-doped ZnO nanocrystals as responsible for observed ferromagnetism.

Fig. 5 shows the ZFC and FC curves for the 5 % Fe doped ZnO nanocrystals. The observed monotonic fall suggests a thermodynamically equilibrium state reminiscent of Curie's law. A small hump at about 60 K may be attributed to presence of ferromagnetic re-entrant behaviour.

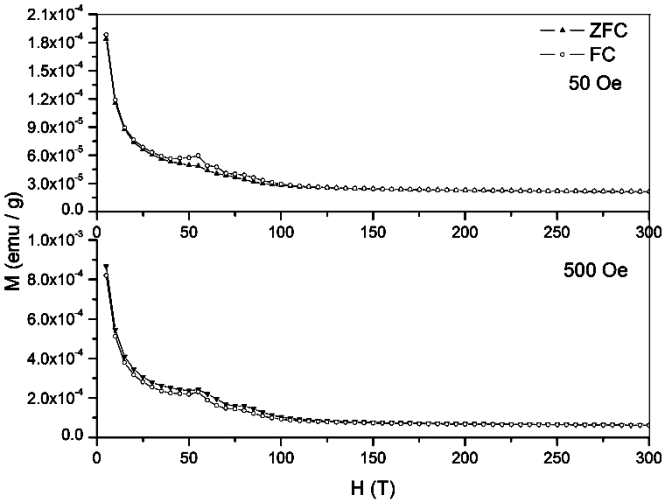

Fig. 5 – Zero field cooled (ZFC) and field cooled (FC) magnetization as a function of temperature for 5 % Fe doped ZnO nanostructures

4. CONCLUSION

The present work was focused on synthesis of transition metal doped ZnO nano crystals in methanol solution at room temperature and their structural, optical and magnetic characterization. Mn, Fe and Ni doped ZnO, doped in composition $x = 0.02$ and 0.05 where synthesized by co-precipitation low entropy method. The crystal structure, magnetic properties and optical properties have been investigated by X-ray diffraction (XRD), SQUID, UV-Visible and PL spectroscopy respectively.

The X-ray diffraction showed that the prepared samples are single phase with the ZnO like wurtzite structure. No secondary phase was found in XRD spectrum. The blue shift in the band gap of transition metal ion doped ZnO was observed in PL emission spectra. A band gap between 3.27 eV to 3.67 eV was calculated for different composition and different transition metal doping by UV Visible spectroscopy. The enhancement of the bang gap energy was attributed to the incorporation of dopant ion into the ZnO host structure.

The magnetic responses the room temperature ferromagnetic properties in 2 % Fe doped, 5 % Ni doped and 2 % Mn doped ZnO. Our analysis suggests that this noticeable ferromagnetism can be attributed to actual incorporation of magnetic ions into the diamagnetic ZnO host structure.

ACKNOWLEDGEMENTS

One of the authors, SM is grateful to AICTE, Govt. of India for financial support for the work.

REFERENCES

1. T. Dietl, H. Ohno, F. Matsukura, J. Cibert, D. Ferrand, *Science* **287**, 1019 (2000).
2. A. Debernardi, M. Fanciulli, *Physica B* **401–402**, 451 (2007).
3. Ü. Özgür, Ya.I. Alivov, C. Liu, A. Teke, M.A. Reshchikov, S. Dogan, V. Avrutin, S.-J. Cho, H. Morkoç, *J. Appl. Phys.* **98**, 041301 (2005).
4. Z.X. Cheng, X.L. Wang, S.X. Dou, K. Ozawa, H. Kimura, P. Munroe, *J. Phys. D: Appl. Phys.* **40**, 6518 (2007).
5. S. Mukherjee, S. Kumar, D. Das, *Nanosci. Nanotech. Lett.* **4**, 110 (2012).
6. S. Mukherjee, D. Das, S. Mukherjee, P.K. Chakrabarti, *J. Phys. Chem. C* **114**, 14763 (2010).
7. N. Singh, R.M. Mehra, A. Kapoor, *J. Nano- Electron. Phys.* **3**, No 1, 132 (2011).
8. I. Balti, A. Mezni, A. Omrani, P. Leone, B. Viana, O. Brinza ,L. Smiri, N. Jouini, *J. Phys. Chem. C* **115**, 15758 (2011).
9. Y. Lei, W. Guozhong, T. Chujuan, W. Hongqiang, Z. Lide, *Chem. Phys. Lett.* **409**, 337 (2005).
10. H.P. Klug, L.E. Alexander, *X-ray diffraction methods for polycrystalline and amorphous materials* (New York: John Wiley and Sons: 1954).
11. M. Nafees, W. Liaqut, S. Ali, M. Shafique, *Appl. Nanosci.* **3**, 49 (2013).
12. Y.S. Wang, P.J. Thomas, P. O'Brien, *J. Phys. Chem. B* **110**, 21412 (2006).
13. M. Hoffman, S. Martin, W. Choi, D. Bahnemann, *Chem. Rev.* **95**, 69 (1995).
14. V.A. Fonoberov, K.A. Alim, A.A. Balandin, Faxian Xiu, Jianlin Liu, *Phys. Rev. B* **73**, 1103 (2006).
15. H.K. Yoshida, K. Sato, *Jpn. J. Appl. Phys. B* **39**, L555 (2000).
P. Radovanovic, D. Gamelin, *Phys. Rev. Lett.* **91**, 157202 (2003)